Supplementary material

Cyclopentadienone-NHC iron(0) complexes as low valent electrocatalysts for water oxidation

Andrea Cingolani,[a] Isacco Gualandi,[a,b]* Erika Scavetta,[a,b] Cristiana Cesari,[a] Stefano Zacchini,[a] Domenica Tonelli,[a,b] Valerio Zanotti,[a,b] Paola Franchi,[c] Marco Lucarini,[c] Emilia Sicilia,[d] Gloria Mazzone,[d] Daniele Nanni,[a] and Rita Mazzoni[a,b]*

[a]Department of Industrial Chemistry "Toso Montanari", University of Bologna, viale Risorgimento, 4 40136 Bologna; [b]Interdipartimental Centre for Industrial Research, Renewable Sources Environment, Sea, Energy (CIRI-FRAME), viale Risorgimento, 4 40136 Bologna, Italia; [c]Department of Chemistry "Giacomo Ciamician", Università di Bologna, via Selmi, 2 40126 Bologna; [d] Department of Chemistry and Chemical Technologies, University of Calabria, Via P. Bucci, 12C, Arcavacata di Rende (CS).

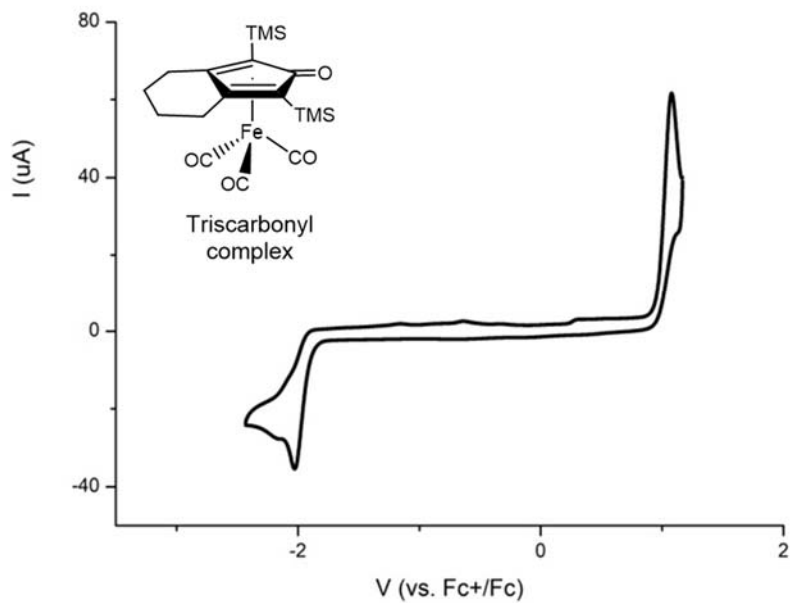## SUMMARY

Cyclic voltammetry characterizations

Figure S1. CV (scan rate = 0.05 V s^{-1}) of triscarbonyl cyclopentadienone iron complex **6**: irreversible redox process at +1.15 V; two irreversible processes in the cathodic side at -2.08 V and -2.60 V.
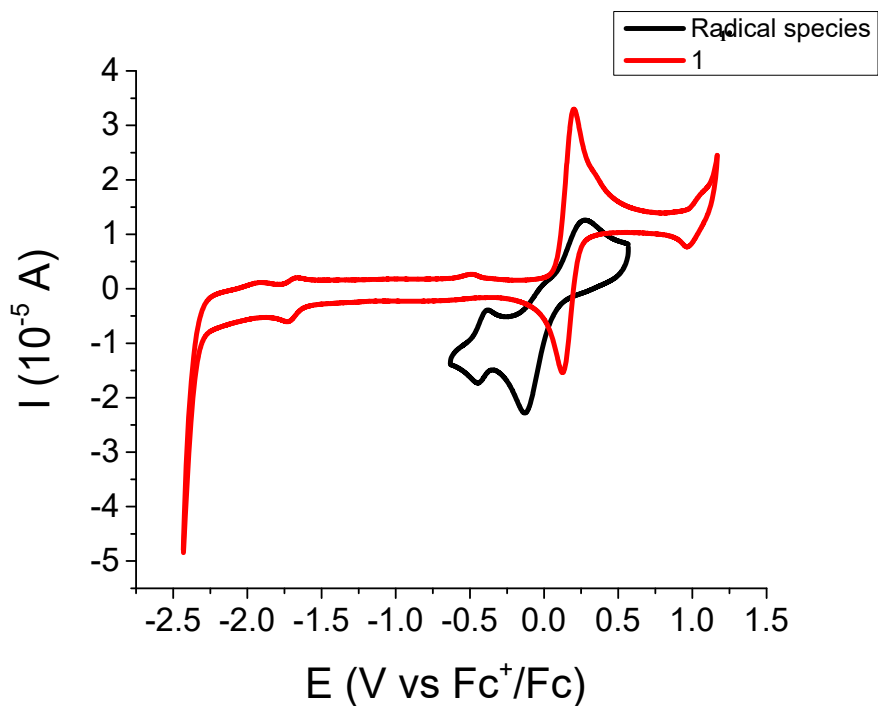
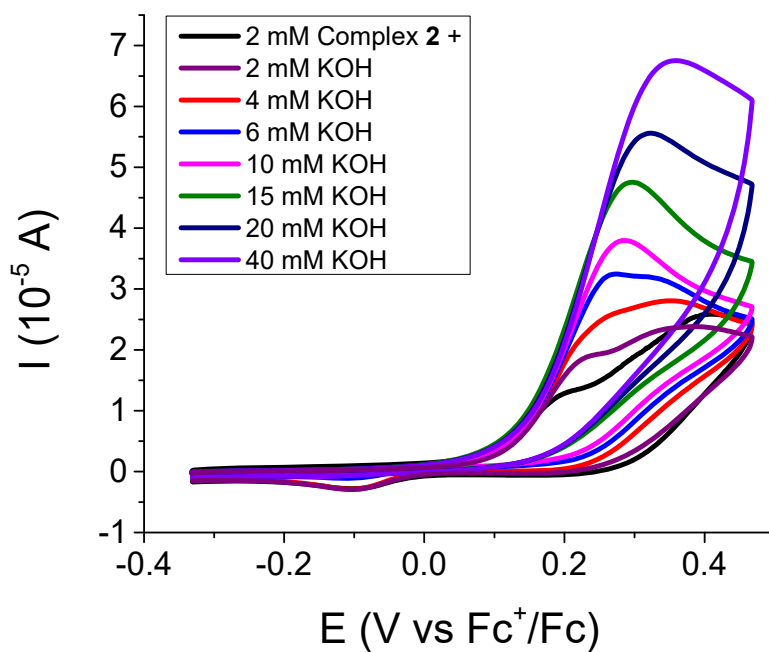**Figure S2.** CVs in 2mM solution of **1** and **1·** at 0.05 V s^{-1}.

Figure S3. CVs in 2 mM solution (THF/H$_2$O, 4:1) of **2** with addition of KOH (scan rate = 0.05 V s^{-1}).
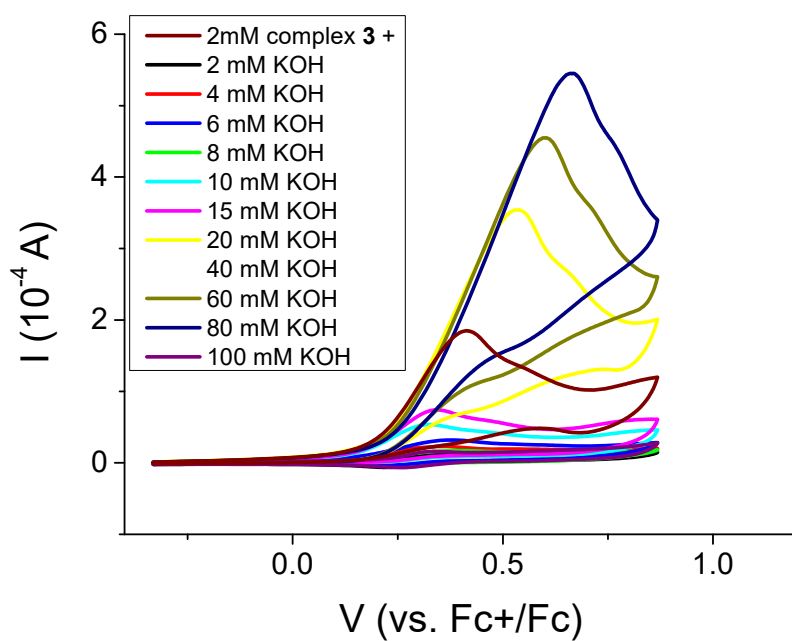
Figure S4. CVs in 2 mM solution (THF/H₂O, 4:1) of **3** with addition of KOH (scan rate = 0.05 V s⁻¹).
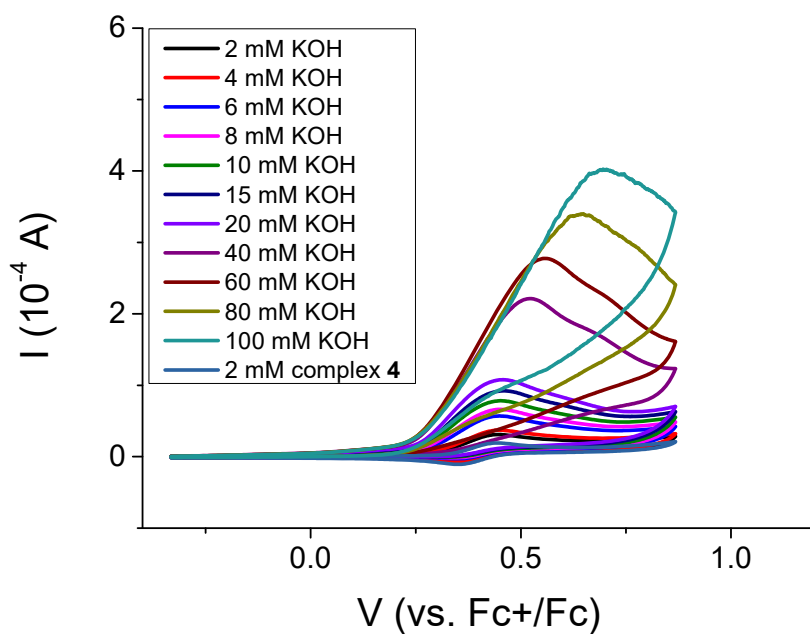

Figure S5. CVs in 2 mM solution (THF/H₂O, 4:1) of **4** with addition of KOH (scan rate = 0.05 V s⁻¹).
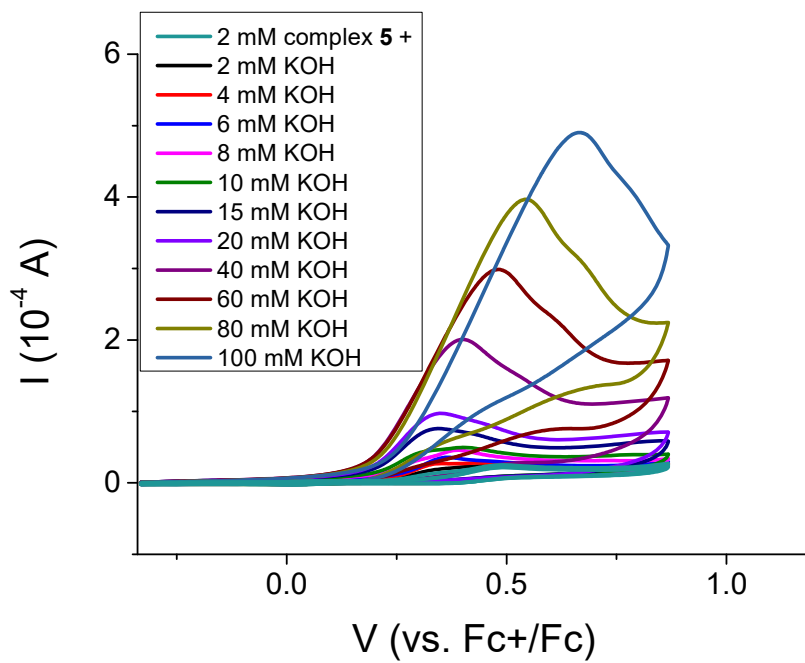
Figure S6. CVs in 2 mM solution (THF/H₂O, 4:1) of **5** with addition of KOH (scan rate = 0.05 V s^{-1}).

Redox behavior of 2 and 5 in THF/H₂O (4:1)

The amino group plays a key role in the redox behavior of complexes **2** and **5**. Taking into accont complex **2** (Figure S6) a first wave which can be considered irreversible is present in the anodic side at a scan rate equal to 0.050 V s⁻¹, together with the main redox peak (II in Figure S6), which displays a backward trace, even if much smaller. The peak potential of the latter has been reported in Table 1 (main text). The backward wave of II increases with the scan rate increase, suggesting the occurrence of a chemical reaction after the electron transfer.[1] Moreover, a new redox wave (III) appears during the second and following cycles which is probably related to a product of the chemical reaction following the electron transfer in II process. Concomitantly, the I redox wave that is always present in the first cycle appears also in the following ones at scan rates equal or lower than 0.020 V s⁻¹ suggesting that it involves a compound which is in equilibrium with the complex.[1] The reaction before the electron transfer is probably of acid-base nature considering that complex **2** contains an amino group. Since process I never exhibits a backward peak, the overall process should be generated by a chemical reaction, followed by an electron transfer that is, in turn, followed by a chemical reaction (CEC mechanism).
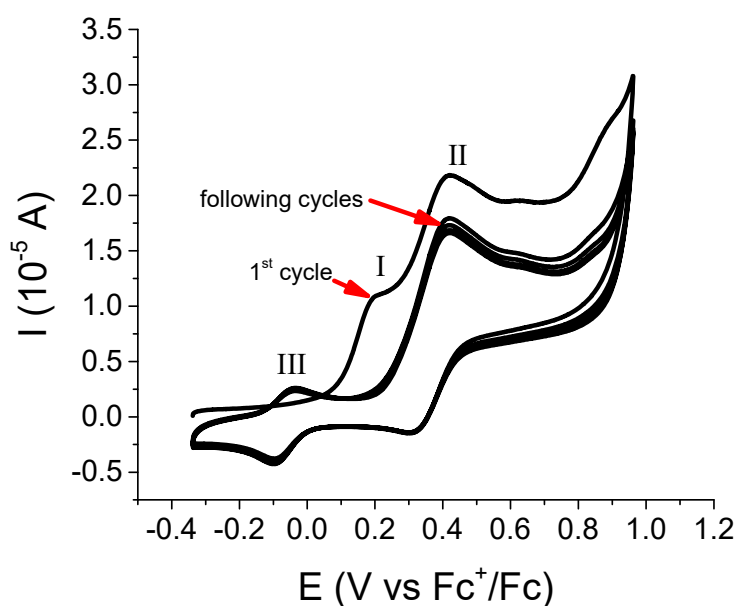

Figure S7 Cyclic voltammogram of **2** recorded at a scan rate of 0.05 V s⁻¹ in THF:H₂O (4:1)
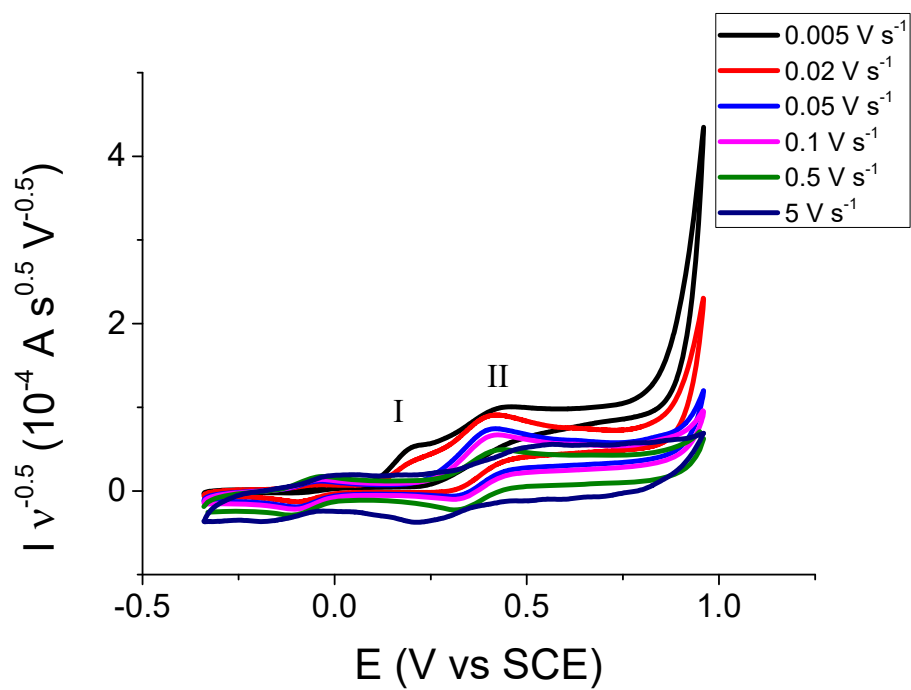
Figure S8 Cyclic voltammograms (reported in normalized current) of **2** recorded at different scan rates in THF:H$_2$O (4:1) after stabilization of the signal.

Foot of the wave analysis: estimation of turn over frequency

The foot of the wave analysis was performed in agreement with the recent literature[2,3,4,5] by exploiting this equation:

$$\frac{i_{cat}}{i_p} = \frac{2.242 n_{cat} (\frac{K_{cat}RT}{Fv})^{\frac{1}{2}}}{1 + e^{(\frac{F}{RT}(E-E^0))}}$$

where n_{cat} is the number of electrons involved in the catalytic reaction, K_{cat} is the pseudo-first-order rate constant, R is the universal gas constant, T is the temperature, F is the Faraday constant, E the potential, E^0 the standard potential of the redox mediator, v is the scan rate, i_{cat} the current recorded in the presence of the substrate and i_b is the peak current of the catalyst in absence of the substrate. The CV of the studied complex was recorded in absence of KOH before carrying out the experiment to study electrocatalysis in order to determine i_b value. I_{cat} vs E curves were recorded in the presence of the substrate in agreement with the procedure described in the experimental section. $\frac{i_{cat}}{i_b}$ values were plotted as a function of $\frac{1}{1 + e^{(\frac{F}{RT}(E-E^0))}}$. Figure S12 shows an example of the graph obtained for the complex **1**. The linear part of the wave was interpolated and the slope resulted:

$$slope = 2.242 n_{cat} (\frac{K_{cat}RT}{Fv})^{\frac{1}{2}}$$

Consequently, K_{cat} can be calculated.

The Turnover frequency (TOF) is related to K_{cat} by the equation:

$$TOF = \frac{2\,K_{cat}}{1 + e^{\left(\frac{F}{RT}(E-E^0)\right)}}$$

When E assume E^0 value, TOF value for O_2 evolution at the standard potential of the used catalyst resulted equal to K_{cat}.

From the slope of the $\frac{i_{cat}}{i_b}$ vs $\frac{1}{1 + e^{(\frac{F}{RT}(E-E^0))}}$ it is possible to calculate K_{cat}, which corresponds to the TOF.
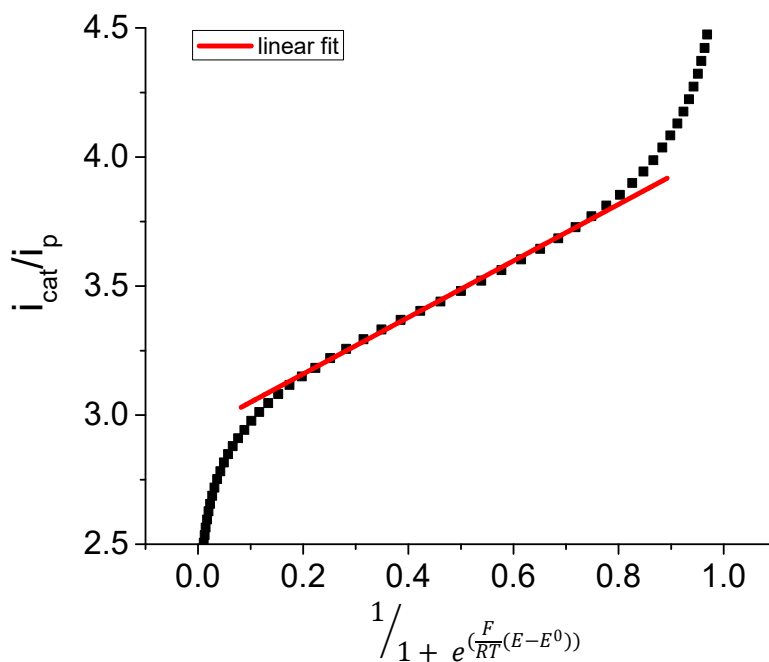
Figure S9. $\frac{i_{cat}}{i_b}$ vs $1\Big/_{1+\,e^{(\frac{F}{RT}(E-E^0))}}$ plot for complex **1**.

Estimation of O$_2$ reduction potential

The thermodynamic potential of O$_2$ reduction during the electrocatalytic experiments was estimated from the Gibbs free energy in THF and water mixture ($\Delta G_{reaction\ (THF)}$).. $\Delta G_{reaction\ (THF)}$ was calculated by the equation:

$\Delta G_{reaction\ (THF)} = \Delta G^0_{reaction(H2O)} - 2\ RT\ ln\ X_{H2O} + 4\ \Delta G_{transfer} + 4\ RT\ ln\ a_{OH-}$

Where $\Delta G^0_{reaction(H2O)}$ is the standard Gibbs free energy of O$_2$ reduction in aqueous environment, X_{H2O} is the molar fraction of water in the mixture, $\Delta G_{transfer}$ is the OH$^-$ free energy for the transfer water to THF:H$_2$O mixture and a_{OH-} is the activity of OH$^-$ that was fixed at 0.01.

$\Delta G^0_{reaction(H2O)}$ was calculated from the standard potential reported by Atkins[6] while $\Delta G_{transfer}$ as reported by Marcus.[7]

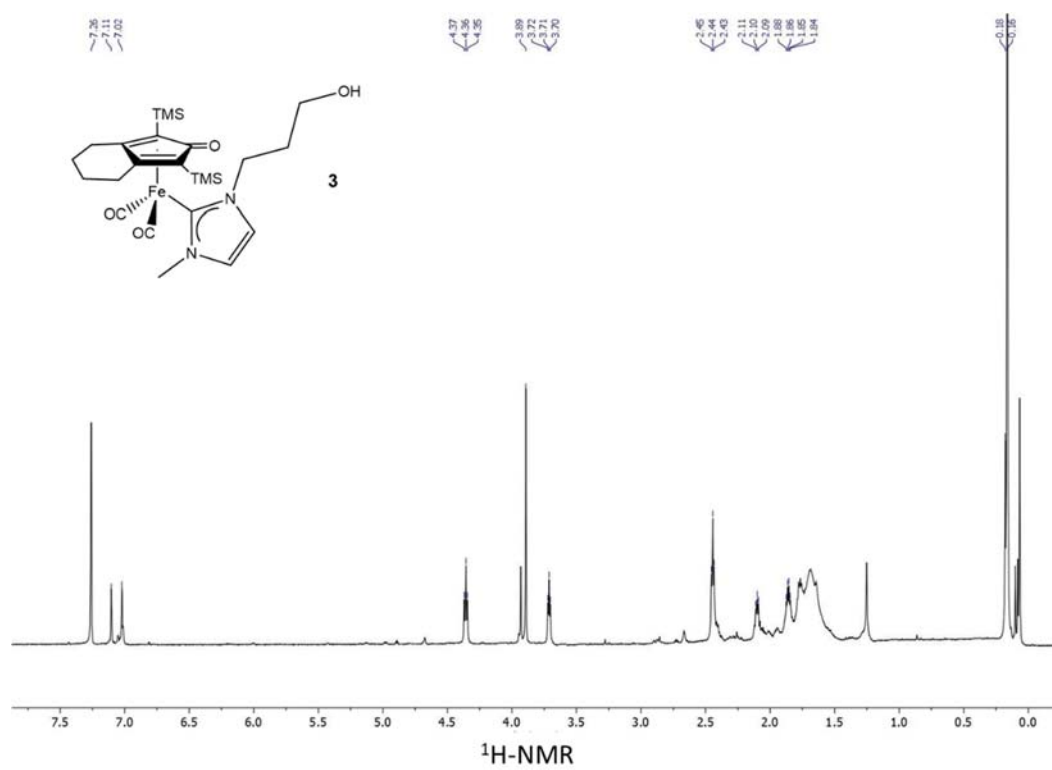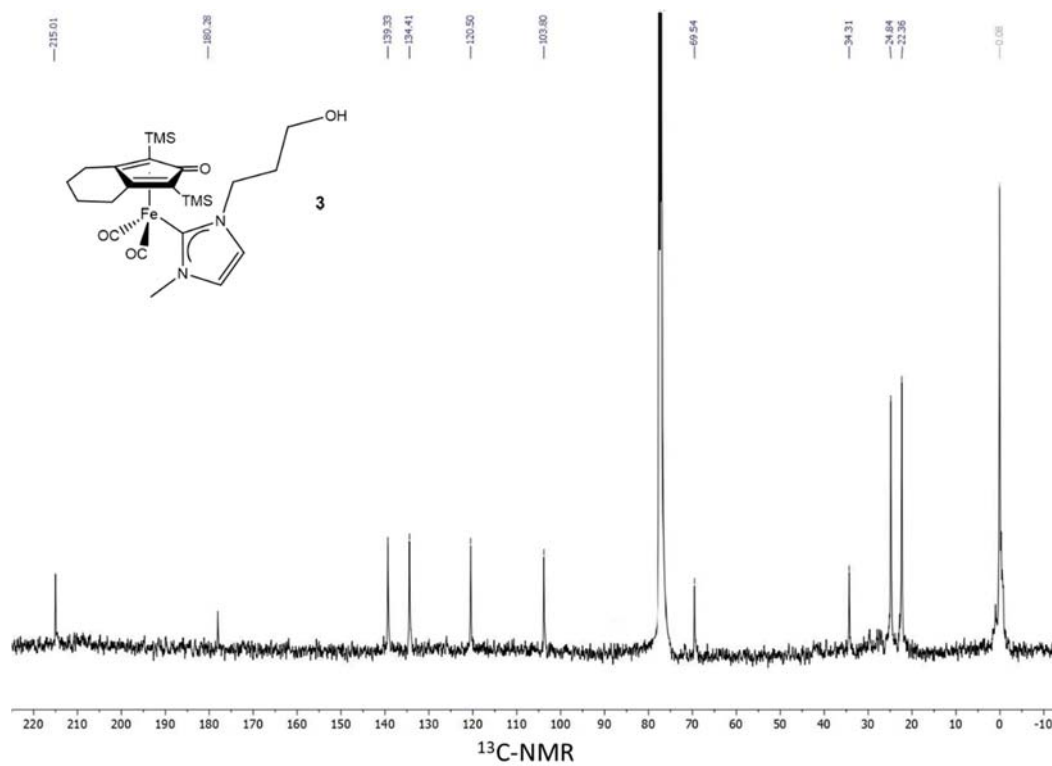**Figure S10.** ^{1}H-NMR of **3**.

Figure S11. ^{13}C-NMR of **3**
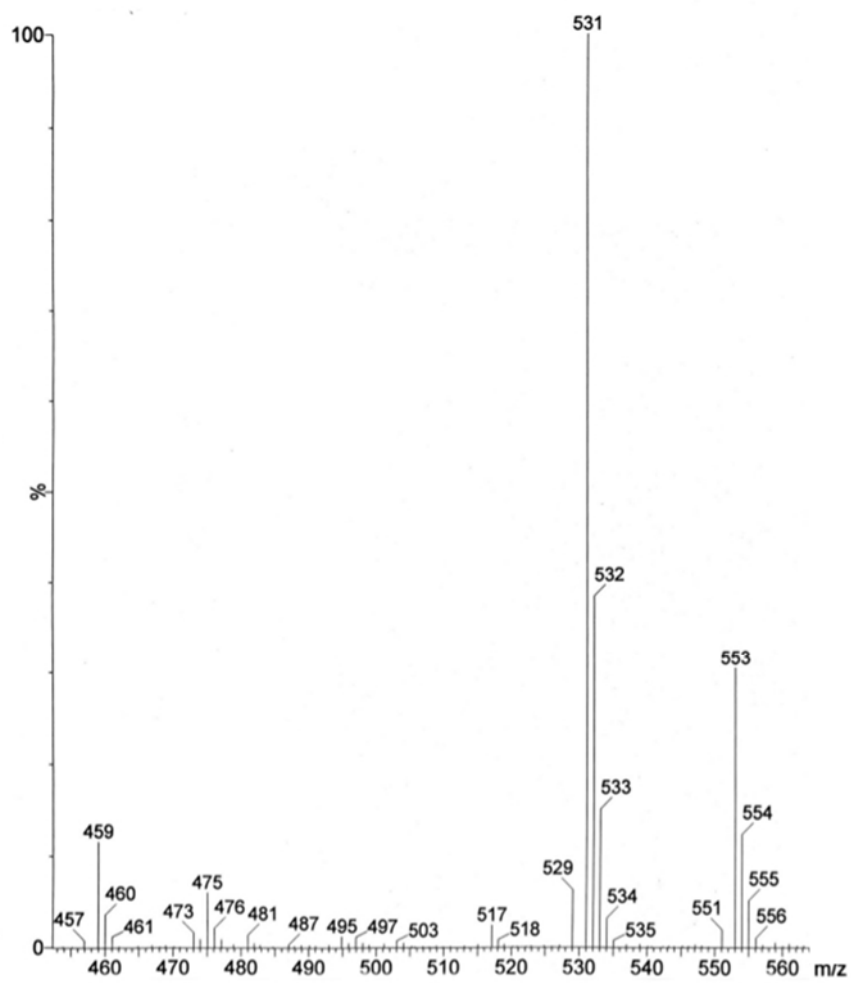
Figure S12. ESI-MS spectrum of **3.**
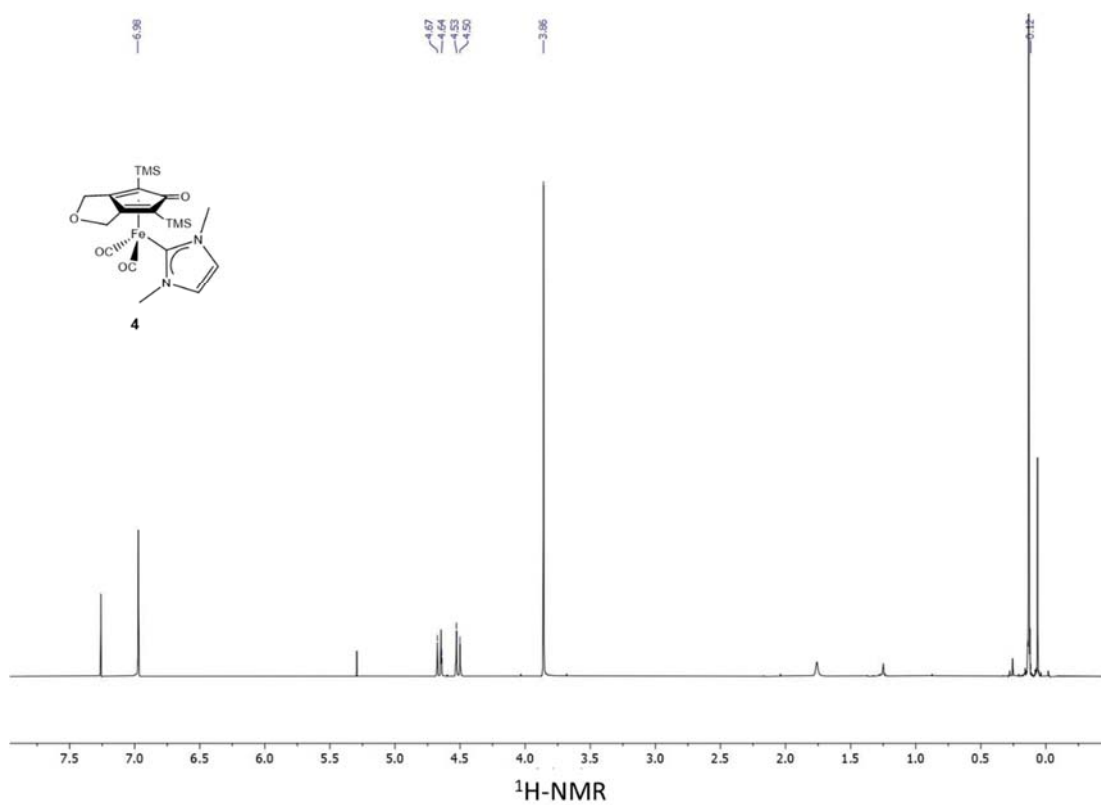
Figure S13. ^{1}H-NMR of **4**.
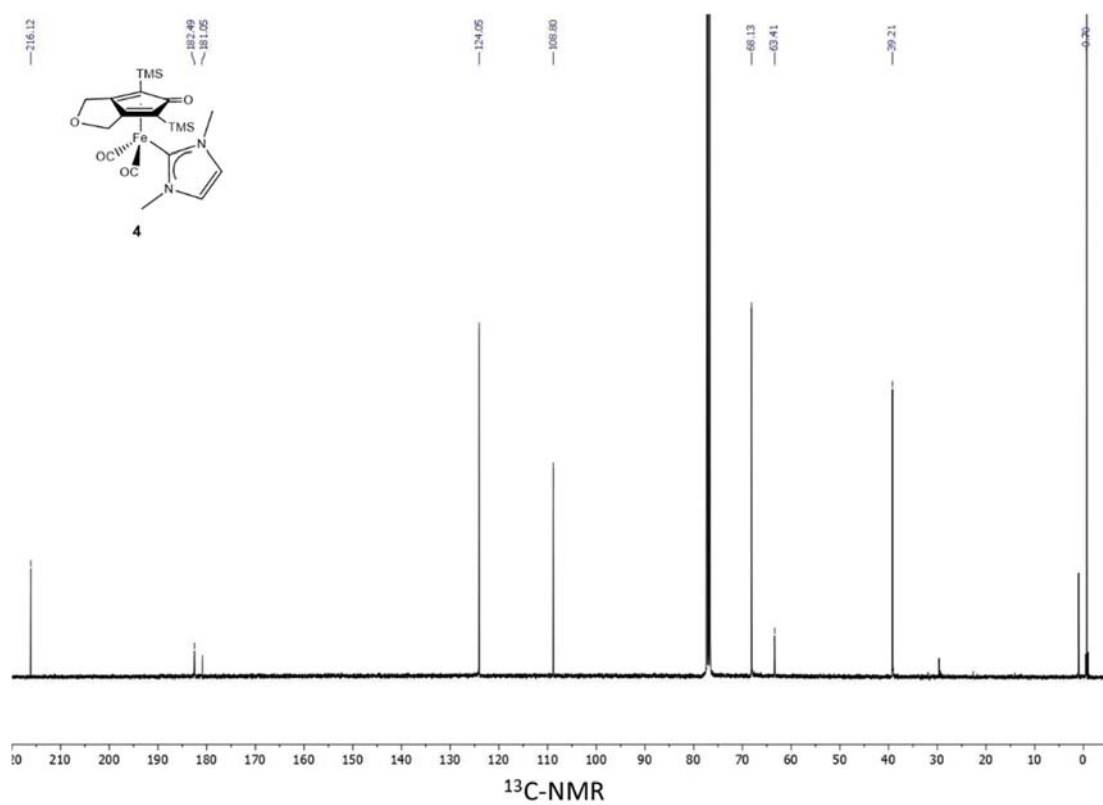
Figure S14. ^{13}C-NMR of **4**.
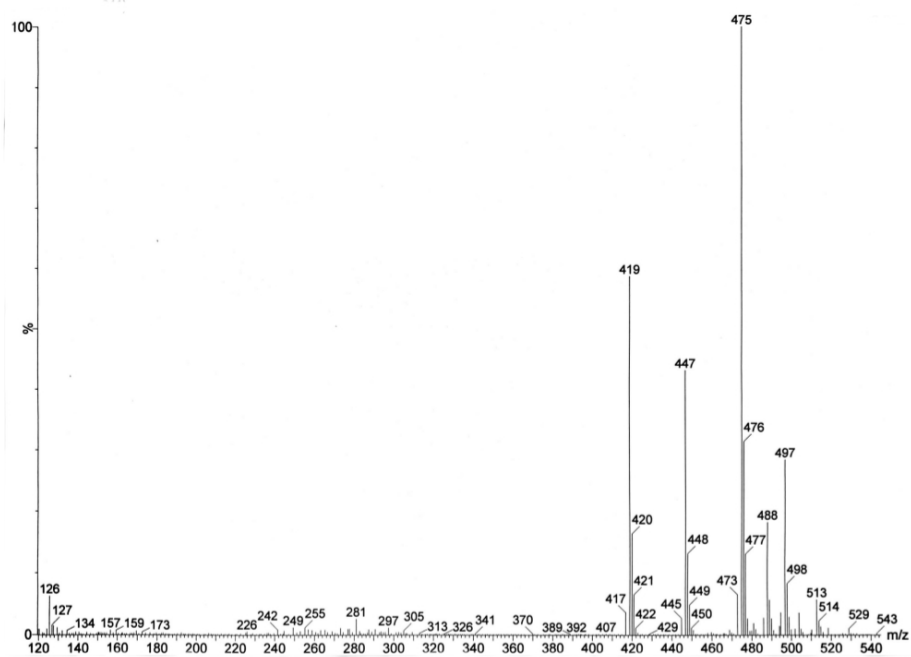
Figure S15. ESI-MS spectrum of **4.**
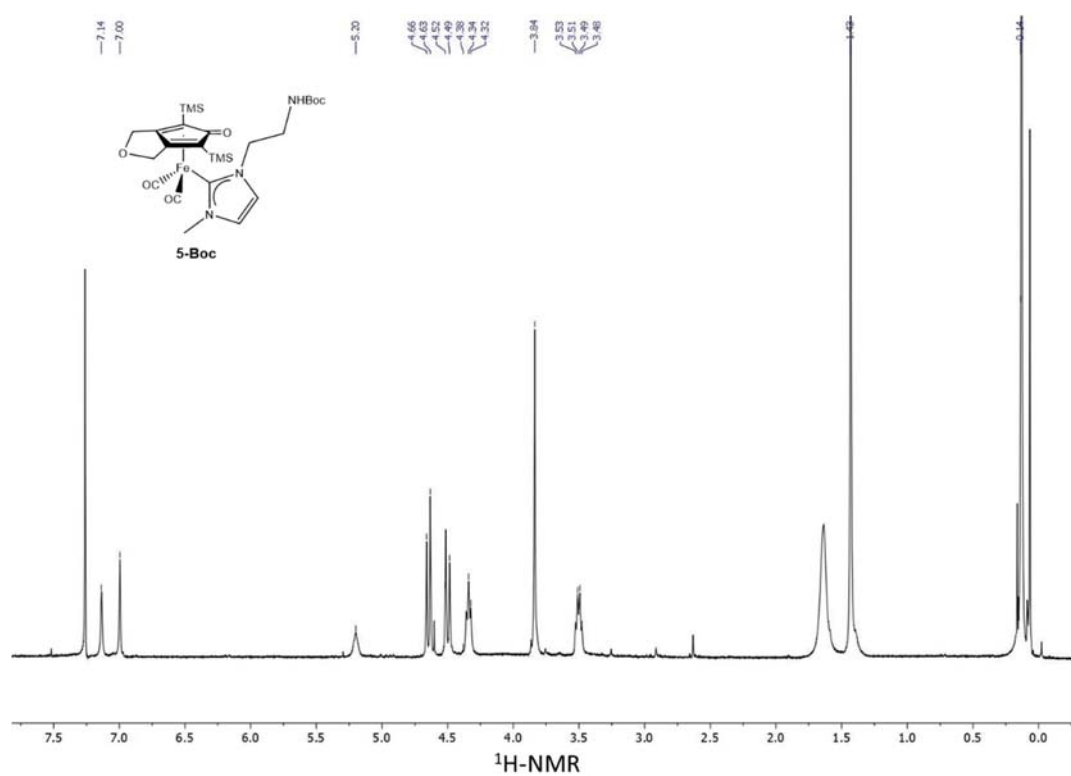
Figure S16. ^{1}H-NMR of **5-Boc.**
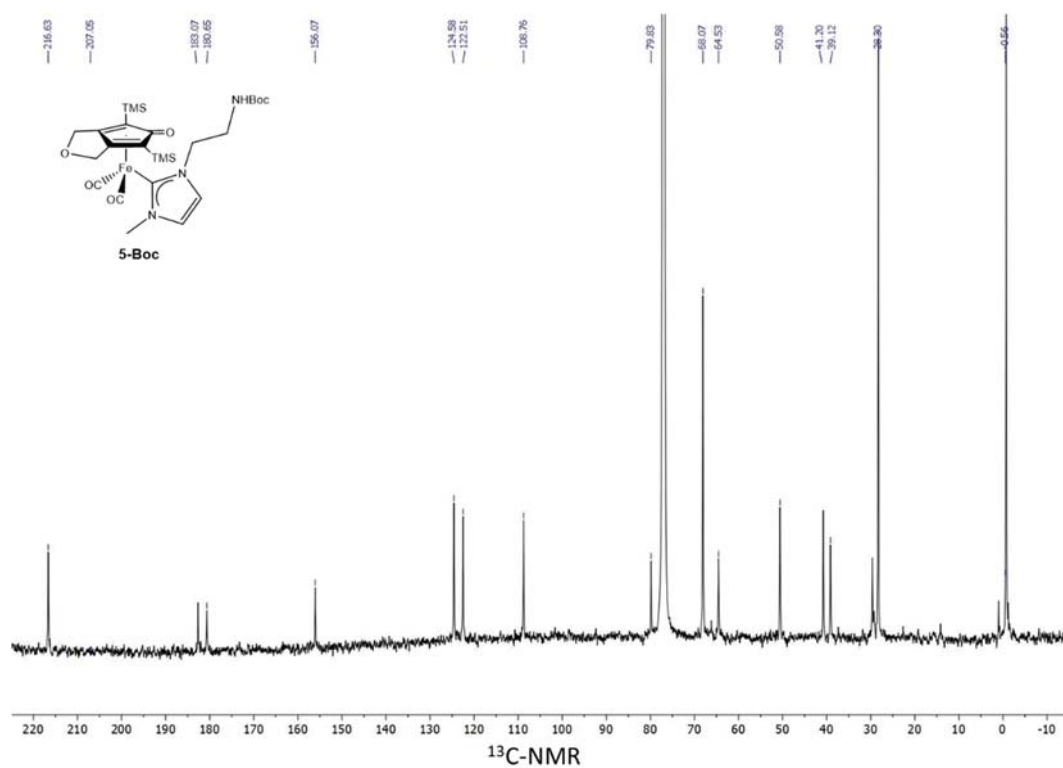
Figure S17. ^{13}C-NMR of **5-Boc.**
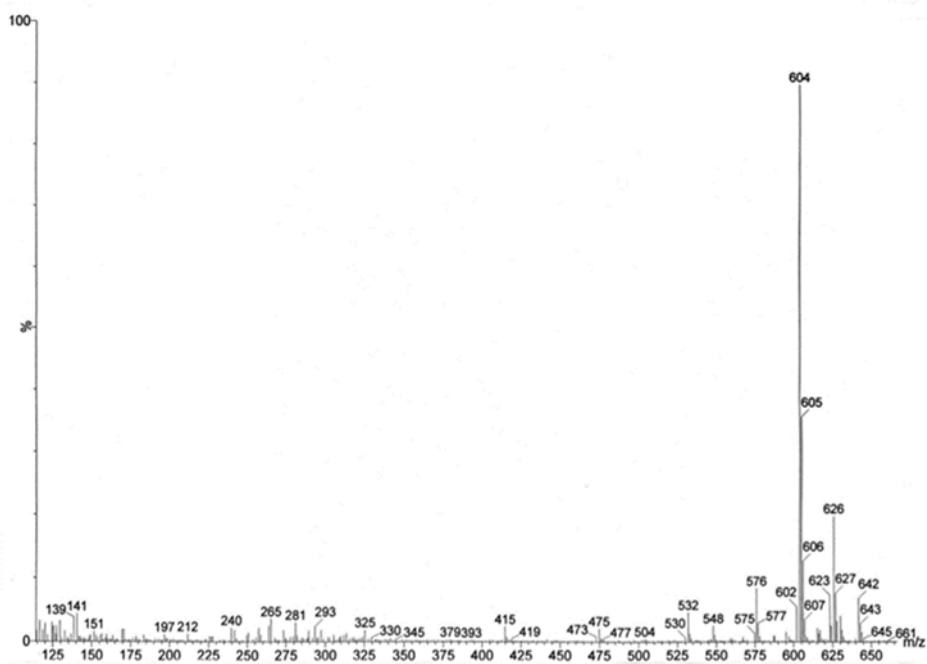
Figure S18. ESI-MS spectrum of **5-Boc.**
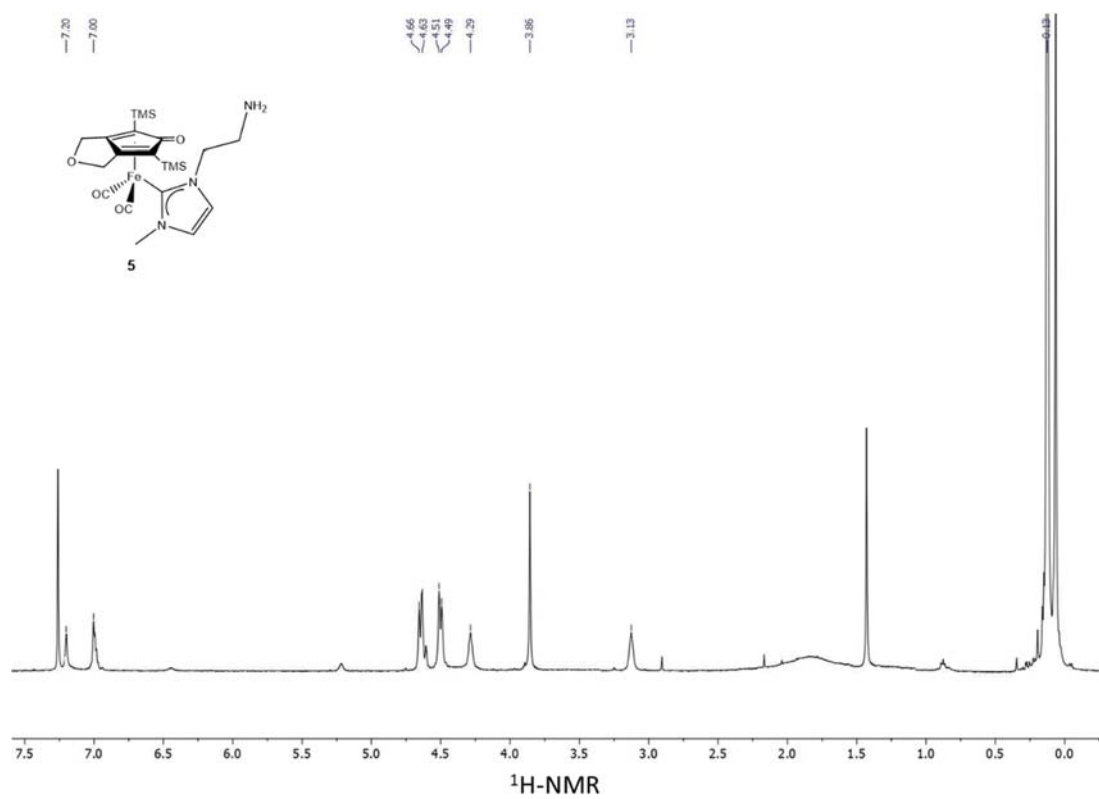
Figure S19. ^{1}H-NMR of **5.**
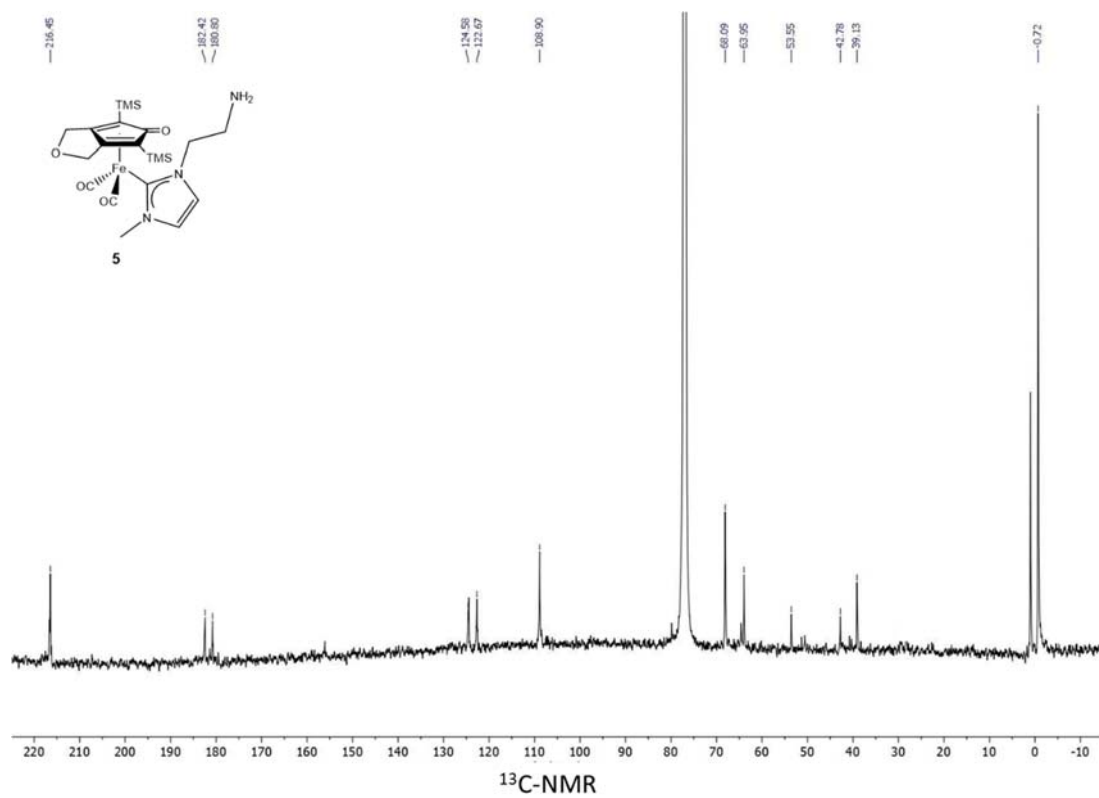
Figure S20. ^{13}C-NMR of **5**.
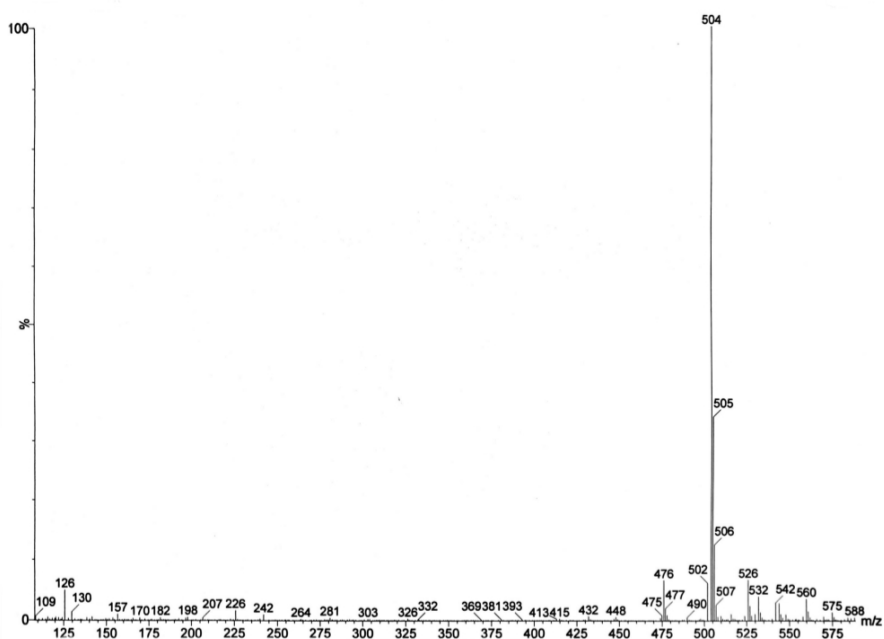
Figure S21. ESI-MS spectrum of **5.**
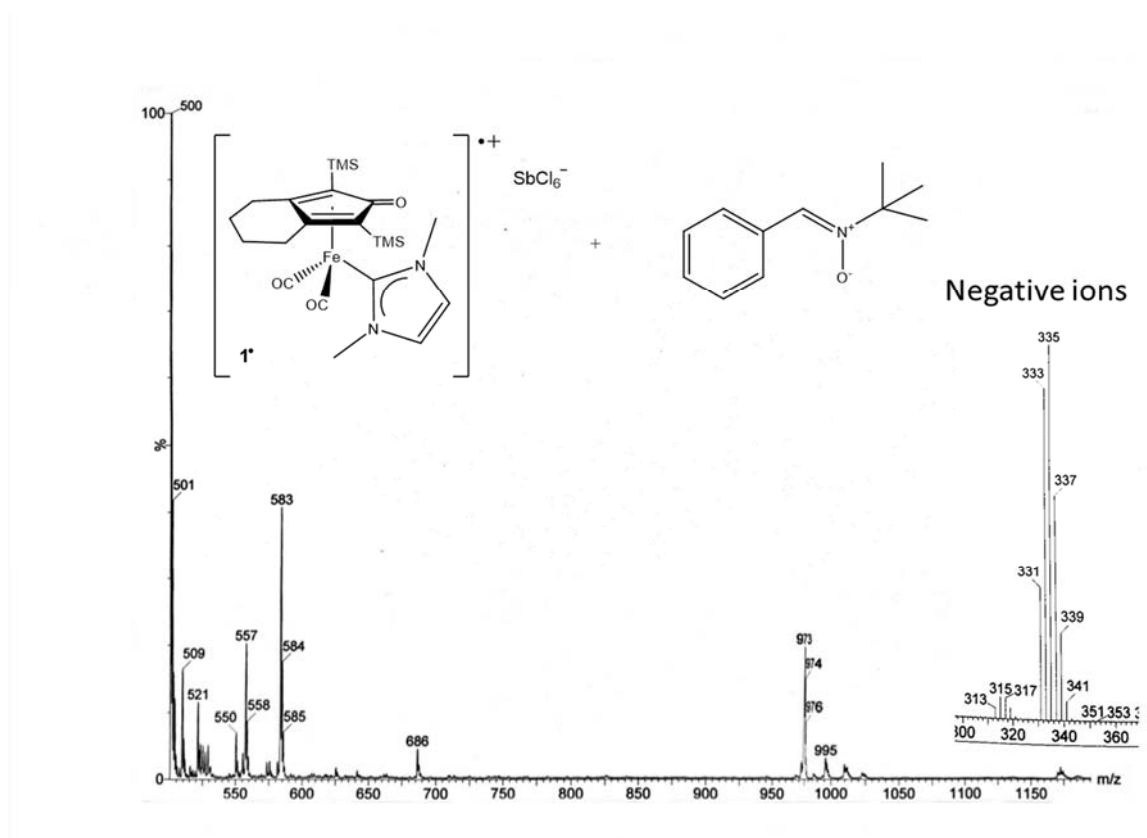
Figure S22. ESI-MS of the **1˙** + spin trap experiment.

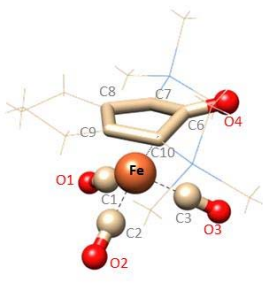S17

EPR characterization of 1˙
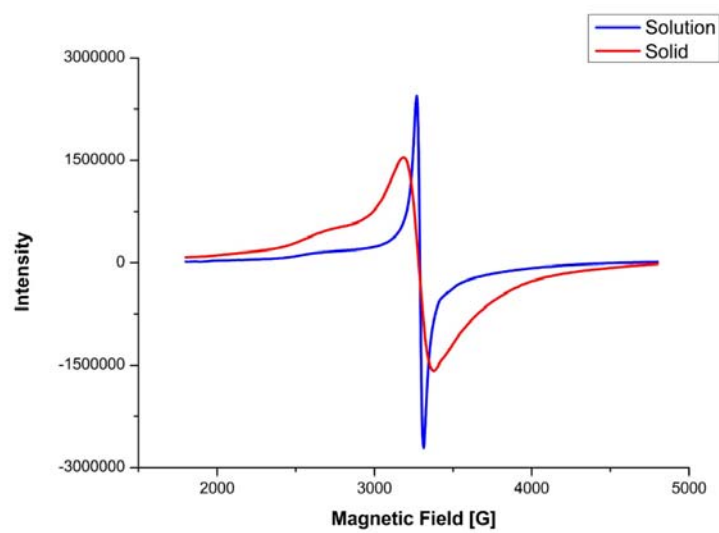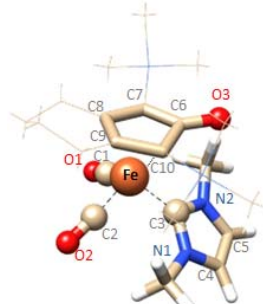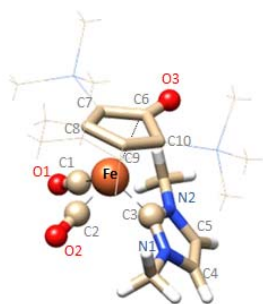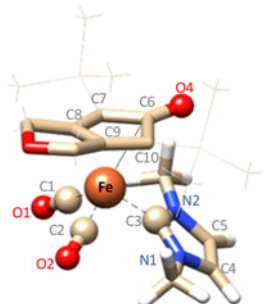
Figure S2. EPR measurement on **1˙** in solid (red line) and THF solution (blu line).

Table S1 Crystal data and experimental details for **4**.

Formula	$C_{20}H_{30}FeN_2O_4Si_2$
Fw	474.49
T, K	100(2)
λ, Å	0.71073
Crystal system	Monoclinic
Space group	$P2_1/n$
a, Å	8.4055(6)
b, Å	18.3319(12)
c, Å	15.0466(10)
β, °	92.570(2)
Cell Volume, Å^3	2316.2(3)
Z	4
D_c, g cm^{-3}	1.361
μ, mm^{-1}	0.782
F(000)	1000
Crystal size, mm	0.21×0.18×0.15
θ limits, °	1.752–27.997
Reflections collected	28207
Independent reflections	5504 [R_{int}= 0.0488]
Data / restraints /parameters	5504 / 0 / 270
Goodness on fit on F^2	1.421
R_1 ($I > 2\sigma(I)$)	0.0751
wR_2 (all data)	0.1319
Largest diff. peak and hole, e Å^{-3}	0.705 / –0.549

Table S2. Most relevant geometrical parameters: bond lengths (Å), valence angles (degrees), together with IRC CO stretching frequencies ν in cm^{-1} for the investigated complexes compared with the available experimental counterparts.

	6	**1**		**1·**	**4**	
Fe-C1	1.790	1.764	*1.747 [a]*	1.801	1.764	*1.767 [a]*
Fe-C2	1.791	1.764	*1.754*	1.842	1.769	*1.778*
Fe-C3	1.807	2.015	*1.996*	2.022	2.013	*1.977*
Fe-C6	2.444	2.408	*2.360*	2.320	2.426	*2.376*
Fe-C7	2.159	2.203	*2.177*	2.181	2.223	*2.171*
Fe-C8	2.106	2.089	*2.067*	2.172	2.074	*2.073*
Fe-C9	2.123	2.153	*2.091*	2.246	2.124	*2.073*
Fe-C10	2.167	2.207	*2.153*	2.266	2.230	*2.139*
C1-O1	1.153	1.159	*1.155*	1.147	1.158	*1.144*
C2-O2	1.153	1.161	*1.153*	1.148	1.159	*1.147*
C3-O3	1.149					
C3-N1	-	1.373	*1.365*	1.365	1.373	*1.361*
C3-N2	-	1.366	*1.360*	1.364	1.366	*1.367*
C6-O4	1.232	1.250	*1.249*	1.236	1.247	*1.241*
C1-Fe-C2	93.6	92.7	*91.5*	90.1	92.8	*95.8*
C1-Fe-C3	98.4	93.4	*97.1*	91.2	93.7	*90.2*
C2-Fe-C3	98.2	98.5	*94.1*	98.4	99.1	*100.0*
Fe-C6-O3	139.3	134.5	*134.1*	129.5	134.2	*136.7*
ν(CO)		2048	1983, 1922[b]	2086 2023[b], 1974[b]	2065	1991, 1931[b]

[a]In italic are crystallographic data; [b]experimental values.

References

[1] Scholz, F. (Ed.) Electrochemical Methods. Guide to Experiment. Springer, Berlin. **2002**.

[2] Costentin, C.; Drouet, S.; Robert, M.; Saveant, J.-M. Turnover Numbers, Turnover Frequencies, and Overpotential in Molecular Catalysis of Electrochemical Reactions. Cyclic Voltammetry and Preparative-Scale Electrolysis, *J. Am. Chem. Soc.* **2012**, *134*, 11235−11242.

[3] Okamura, M.; Kondo, M.; Kuga, R.; Kurashige, Y.; Yanai, T.; Hayami, S.; Praneeth, V. K.; Yoshida, M.; Yoneda, K.; Kawata, S.; Masaoka, S. A pentanuclear iron catalyst designed for water oxidation *Nature* **2016**, *530*, 465-468.

[4] Song, N.; Concepcion, J. J.; Binstead, R. A.; Rudd, J. A.; Vannucci, A. K.; Dares, C. J.; Coggins, M. K.; Meyer, T. J. Base-enhanced catalytic water oxidation by a carboxylate–bipyridine Ru(II) complex, PNAS **2015**, *112*, 4935-4940.

[5] Bard, A. J.; Faulkner, L. R. Electrochemical Methods, Fundamentals and Applications, 2nd Edn. New York, NY:Wiley. **2000**.

[6] Atkins, P. (1997). Physical Chemistry, 6th edition (W.H. Freeman and Company, New York).

[7] Marcus, Y. Gibbs Energies of Transfer of Anions from Water to Mixed Aqueous Organic Solvents, *Chem. Rev.*, **2007**, *107*, 3880−3897.